JID Open

Suppression of Hyperactive Immune Responses Protects against Nitrogen Mustard Injury

Liemin Au[1,2], Jeffrey P. Meisch[1,8], Lopa M. Das[1,8], Amy M. Binko[1], Rebecca S. Boxer[3], Amy M. Wen[4], Nicole F. Steinmetz[4,5,6,7] and Kurt Q. Lu[1]

DNA alkylating agents like nitrogen mustard (NM) are easily absorbed through the skin and exposure to such agents manifest not only in direct cellular death but also in triggering inflammation. We show that toxicity resulting from topical mustard exposure is mediated in part by initiating exaggerated host innate immune responses. Using an experimental model of skin exposure to NM we observe activation of inflammatory dermal macrophages that exacerbate local tissue damage in an inducible nitric oxide synthase (iNOS)-dependent manner. Subsequently these activated dermal macrophages reappear in the bone marrow to aid in disruption of hematopoiesis and contribute ultimately to mortality in an experimental mouse model of topical NM exposure. Intervention with a single dose of 25-hydroxyvitamin D3 (25(OH)D) is capable of suppressing macrophage-mediated iNOS production resulting in mitigation of local skin destruction, enhanced tissue repair, protection from marrow depletion, and rescue from severe precipitous wasting. These protective effects are recapitulated experimentally using pharmacological inhibitors of iNOS or by compounds that locally deplete skin macrophages. Taken together, these data highlight a critical unappreciated role of the host innate immune system in exacerbating injury following exposure to NM and support the translation of 25(OH)D in the therapeutic use against these chemical agents.

Journal of Investigative Dermatology (2015) **135,** 2971–2981; doi:10.1038/jid.2015.322; published online 10 September 2015

INTRODUCTION

Mustard gas and mustard-related compounds are vesicating agents that, on skin exposure, cause severe epithelial and deep tissue injury characterized by blistering, acute inflammation, induration, and edema (Requena *et al.*, 1988; Sharma *et al.*, 2010a; Sharma *et al.*, 2010b). Historically, these powerful vesicants were exploited as chemical warfare agents during World War I and later conflicts (Pearson, 2006). Through its action as a DNA alkylating agent, nitrogen mustard (NM) and related compounds like nitrosourea, chlorambucil, and estramustine phosphate generate DNA strand breaks with consequent cell death, a unique property that was exploited and adapted in medicine as effective therapy against rapidly proliferating cancer cells (DeVita and Chu, 2008). However, its clinical utility is limited by its dose-dependent toxicity (DeVita and Chu, 2008).

On exposure, NM is absorbed through skin and re-deposited in subcutaneous fat to inflict tissue destruction directly from the alkylating effects of NM. Injured tissue creates an inflammatory foci (Keramati *et al.*, 2013), (Gunnarsson *et al.*, 1991) to attract neutrophils, monocytes, and macrophages (Jain *et al.*, 2014). Persistence of the initial inflammatory phase can amplify an immune response and induce further tissue injury (Laskin *et al.*, 1996a; Laskin and Laskin, 1996; Laskin *et al.*, 1996b; Kondo and Ishida, 2010). NM-induced wounds generate oxidative and nitrosative stress to exacerbate tissue destruction (Yaren *et al.*, 2007; Zheng *et al.*, 2013). We and others have shown that inducible nitric oxide synthase (iNOS)-producing hyper-activated macrophages delay wound repair and exaggerate wound pathogenesis (Cash *et al.*, 2014; Das *et al.*, 2014). Therefore therapeutic intervention(s) targeting these inflammatory cells may be a suitable strategy to subdue inflammatory damage. The use of pharmacologic inhibitors of iNOS, though efficacious in experimental animal models, has limited translation clinically due to cytotoxicity and adverse off-target physiological effects on circulatory function (Laskin *et al.*, 1996b; Bogdan, 2001; Malaviya *et al.*, 2012). Consequently, we focused on

[1]*Department of Dermatology, Case Western Reserve University, Cleveland, Ohio, USA;* [2]*Department of Chemical Engineering, Case Western Reserve University, Cleveland, Ohio, USA;* [3]*Department of Medicine, University of Colorado School of Medicine, Denver, Colorado, USA;* [4]*Department of Biomedical Engineering, Case Western Reserve University, Cleveland, Ohio, USA;* [5]*Department of Radiology, Case Western Reserve University, Cleveland, Ohio, USA;* [6]*Department of Material Science and Engineering, Case Western Reserve University, Cleveland, Ohio, USA and* [7]*Department of Macromolecular Science and Engineering, Case Western Reserve University, Cleveland, Ohio, USA*

Correspondence: Kurt Q. Lu, Department of Dermatology, Case Western Reserve University, 10900 Euclid Avenue, Biomedical Research Building Room 529, Cleveland, Ohio 44106, USA. E-mail: kurt.lu@case.edu

[8]*These authors contributed equally to this work and should be considered as second authors.*

Abbreviations: BM, bone marrow; CBC, complete blood count; NM, nitrogen mustard; 25(OH)D, 25-hydroxyvitamin D3; iNOS, inducible nitric oxide synthase

Received 5 February 2015; revised 4 June 2015; accepted 23 June 2015; accepted article preview online 19 August 2015; published online 10 September 2015

Vitamin D3, a hormone that has acquired recognition as an immunomodulator through direct inhibition of NFκB activation and suppression of TNF-α and iNOS expression (Cohen-Lahav, 2006; #9; Holick, 1993, 2003; Chen *et al.*, 2011; Lagishetty *et al.*, 2011). Typically, the kidneys control the rate limiting step in converting circulating 25-hydroxyvitamin D3 (25(OH)D), the inactive form of vitamin D3, into calcitriol, the active form (1,25α$(OH)_2$D). The ability of macrophages to perform this conversion by virtue of its intracellular enzyme CYP27A1 (Mora *et al.*, 2008) allowed us to hypothesize that 25(OH)D should effectively block macrophage-mediated iNOS upregulation and confer protection from exacerbated local and systemic tissue injury that follows NM exposure.

This study investigates a NM skin wound model that demonstrates a critical role for activated cutaneous macrophages in delaying wound healing and causing disruption of hematopoiesis via iNOS production. The model emphasizes the therapeutic efficacy of 25(OH)D intervention to counteract an acute immune response that exacerbates NM-mediated pathology and enables repopulation of bone marrow (BM) cells. We determine that topical application of NM activates cutaneous macrophages to produce iNOS that traffic to the BM and cause further disruption of hematopoiesis. A single administration of 25(OH)D promotes survival by moderating the immune response and restoring blood cell loss and BM depletion.

RESULTS

25(OH)D prevents NM-mediated tissue destruction by antagonizing macrophage-derived iNOS

We established a NM-skin contact model characterized by topical (percutaneous) application of NM to an 8 mm diameter (50 mm^2) circular template on the dorsal skin of C57BL/6J mice, herein referred to as wound area. Working on the hypothesis that elevated macrophage-derived iNOS is the stimulus for exacerbated tissue injury following NM exposure led us to explore whether 25(OH)D can effectively counteract NM-induced iNOS. One hour following NM exposure, an intraperitoneal (i.p.) bolus of 5 ng 25(OH)D was administered. We show that NM-induced wound appears on the first day and increases progressively over time. Treatment with 25(OH)D or a specific pharmacological inhibitor of iNOS (compound 1400W, 10 mg kg^{-1}) delays hemorrhagic crust formation and eventually resolves wound by day 19 (data not shown) (Figure 1a). In both treatment intervention groups, the surrounding skin appeared healthy with full recovery of hair regrowth and a small residual scar by day 40. Gross wound images correlated with a percentage wound area size relative to the initial 50 mm^2 template (Figure 1b). Histological examination of skin at the corresponding time point in mice not treated with either 25(OH)D or 1400W intervention reveal full-thickness necrosis, robust inflammation, and edema following NM contact. Skin from NM+25(OH)D mice displayed a milder histological phenotype with diminished inflammatory infiltrates, skin necrosis limited to the epidermis and superficial dermis with preservation of deep skin structures including hair follicles, subcutaneous fat, and panniculus carnosus (Figure 1c). Furthermore, a similar protection from exacerbated skin damage was also observed with iNOS inhibition using compound 1400W (Figure 1a–c). The protective effect of 25(OH)D is not strain specific, as similar results were observed using BALB/c mice (Supplementary Figure S1a–c online). Exacerbation of skin necrosis was associated with elevated levels of skin specific iNOS and TNFα mRNA 48 hours post NM exposure, that was significantly reduced by intervention with 25(OH)D (Figure 1d, Supplementary Figure S1d online). This was consistent with results using *nos2*$^{-/-}$ mice, which exhibit mild inflammatory response to NM with preservation of the skin layers, deep skin structures and minimal tissue destruction (Supplementary Figure S1e online). Since iNOS is primarily produced by inflammatory macrophages and monocytes, confocal microscopy was performed to co-localize F4/80+/iNOS+ macrophages infiltrating the wound bed that were significantly diminished with 25(OH)D intervention (Figure 1e).

To demonstrate a role for dermal macrophages in delaying wound healing, the latter were depleted by intradermal injection with liposomal clodronate 1 hour after NM exposure (Ward *et al.*, 2011). We observed dramatic reduction of skin wound with sparse inflammation and edema (Figure 1f) corresponding to accelerated skin wound healing. Consistent with reduced skin wound area, clodronate treatment protected animals from disruption of skin architecture (Figure 1g) and mice exhibited significantly diminished iNOS (Figure 1h) and TNFα (Supplementary Figure S1f online) mRNA expression, supporting the hypothesis that hyperactive dermal macrophages may be the source of exacerbated cutaneous destruction.

25(OH)D rescues mice from systemic effects of NM

Injury from NM exposure is known to cause systemic damage especially to adipose-rich tissue such as the BM leading to morbidity and mortality (Schein *et al.*, 1987). Our experimental model of NM exposure (26.6 mg kg^{-1}) was developed based on a dose response (Supplementary Figure S2a online). Daily evaluation of animal well-being showed that by day 4, NM caused severe morbidity including hunched posture and statistically significant precipitous loss of body weight by almost 30% (Figure 2a). At this exposure dose, mortality (either observed or meeting weight loss criteria for compassionate euthanasia) was observed in 90% of mice between days 4 and 13 in contrast to mice that received 25(OH)D intervention (Kaplan–Meier survival plot), (Figures 2b, $P<0.001$, log-rank test). Examination of whole blood by complete blood count (CBC) analysis (Table 1) shows acute anemia and lymphopenia with visible loss of cells on peripheral blood smears (Figure 2c). Intervention with 25(OH)D or 1400 W restored blood cell counts comparable to healthy controls (Figure 2c, Table 1). Disruption of the hematopoietic compartment was characterized by acute loss of cellularity selectively in the BM (Figure 2d) with no observed overt histologic abnormalities in the visceral organs (Supplementary Figure S2b online), suggesting compartmental specificity of NM-mediated effects in our experimental model.

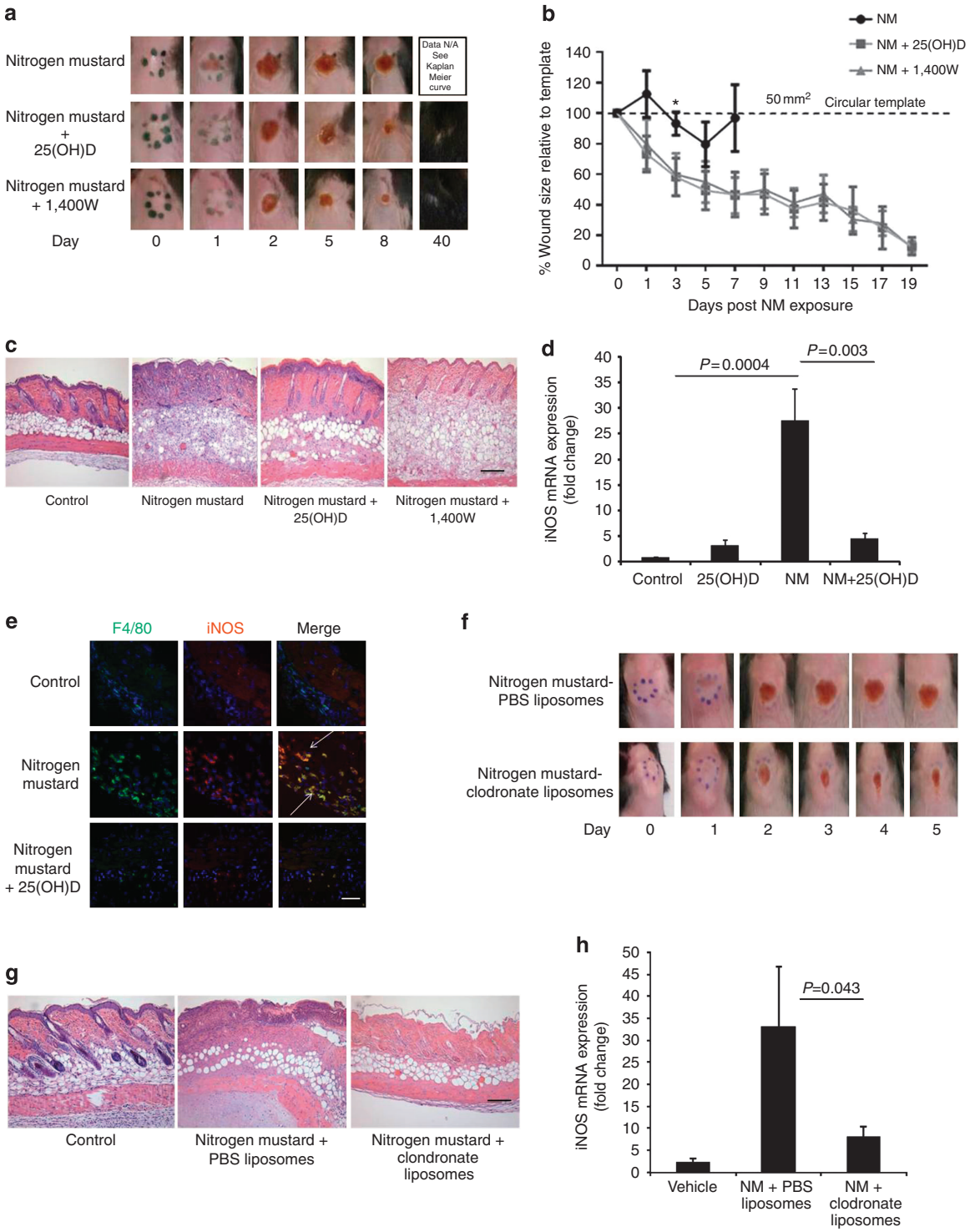

Figure 1. 25(OH)D protects mice from NM-induced skin erosions. Circular mouse skin (50 mm^2) biopsies were obtained 48 hours following topical NM exposure in presence and absence of 25(OH)D and compound 1400W for (**a**) representative images of NM-induced skin injury, (**b**) wound sizes measured relative to 50 mm^2 circular template (*$p = 0.042$) ($n = 5$) (**c**) histological images to assess NM-mediated skin necrosis and (**d**) detection of iNOS mRNA expression ($n = 9$; $P < 0.003$), (**e**) detection of activated macrophages by co-localization of iNOS (red) and F4/80+ (green) macrophages (indicated with arrows) using confocal microscopy. Mice were injected with clodronate liposomes or PBS liposomes following topical application of NM and 48 hours post exposure (**f**) imaged for wound regression, (**g**) histological assessment of skin injury and (**h**) detection of iNOS mRNA expression ($n = 4$; $P < 0.043$). All data presented as means ± SEM. Scale Bar = 100 μm.

Depletion of BM cells was not mouse strain specific as BALB/c mice exhibited similar BM histopathology (Supplementary Figure S2c online).

25(OH)D intervention facilitates recovery of BM cells from acute lymphopenia

Acute loss of BM cellularity on day 5 post exposure prompted us to examine the BM compartment immediately following cutaneous NM exposure. Enumeration of BM cells revealed that very early on, the alkylating effects of NM precipitates in an acute drop of cellularity by days 1 and 2 irrespective of intervention with 25(OH)D. Days 3 through 5 mark a recovery of total BM cell numbers in animals with 25(OH)D intervention (Figure 3a). Examination of BM cells by flow cytometric analysis show significant loss of nucleated cells in the leukocyte gate on day 5 post NM exposure, in contrast to animals that received intervention with 25(OH)D (30.4 ± 9.8% vs. 85.2 ± 1.1%; Figure 3b). Furthermore a relative increase (2.5-fold) in F4/80+ macrophages was observed in NM exposed mice compared with controls (54.5 ± 3.71% vs. 24.8 ± 2.48%; Figure 3c). Taking into account that NM exposure results in global loss of BM cells, enumeration of absolute numbers of F4/80+ cells reveal fewer cell counts from NM compared with other treatment conditions (Supplementary Figure S3 online). 25(OH)D treatment effectively reduced the percentage of F4/80+ numbers back to

Table 1. CBC analyses of 25(OH)D treated mice on day 5 post NM exposure 1400W ($n = 9$)

	Control	NM	NM+25(OH)D	NM+1400W
WBC ($\times 10^3\ \mu l^{-1}$)	13.53 ± 4.83	3.62 ± 2.25*	10.35 ± 4.53*	6.95 ± 7.28
HCT (%)	43.13 ± 4.06	24.47 ± 6.27*	41.17 ± 6.41*	37.36 ± 4.52*
LYM ($\times 10^3\ \mu l^{-1}$)	10.65 ± 4.10	2.65 ± 1.65*	7.43 ± 3.08*	4.68 ± 4.38
MONO ($\times 10^3\ \mu l^{-1}$)	0.70 ± 0.24	0.21 ± 0.16*	0.65 ± 0.28*	0.45 ± 0.50
GRAN ($\times 10^3\ \mu l^{-1}$)	2.18 ± 0.68	0.70 ± 0.49*	2.27 ± 1.41*	1.83 ± 2.47

Abbreviations: 25(OH)D, 25-hydroxyvitamin D3; CBC, complete blood count; GRAN, granulocytes; HCT, hematocrit; LYM, lymphocytes; MONO, monocytes; NM, nitrogen mustard; WBC, white blood cell.
*$P < 0.01$.

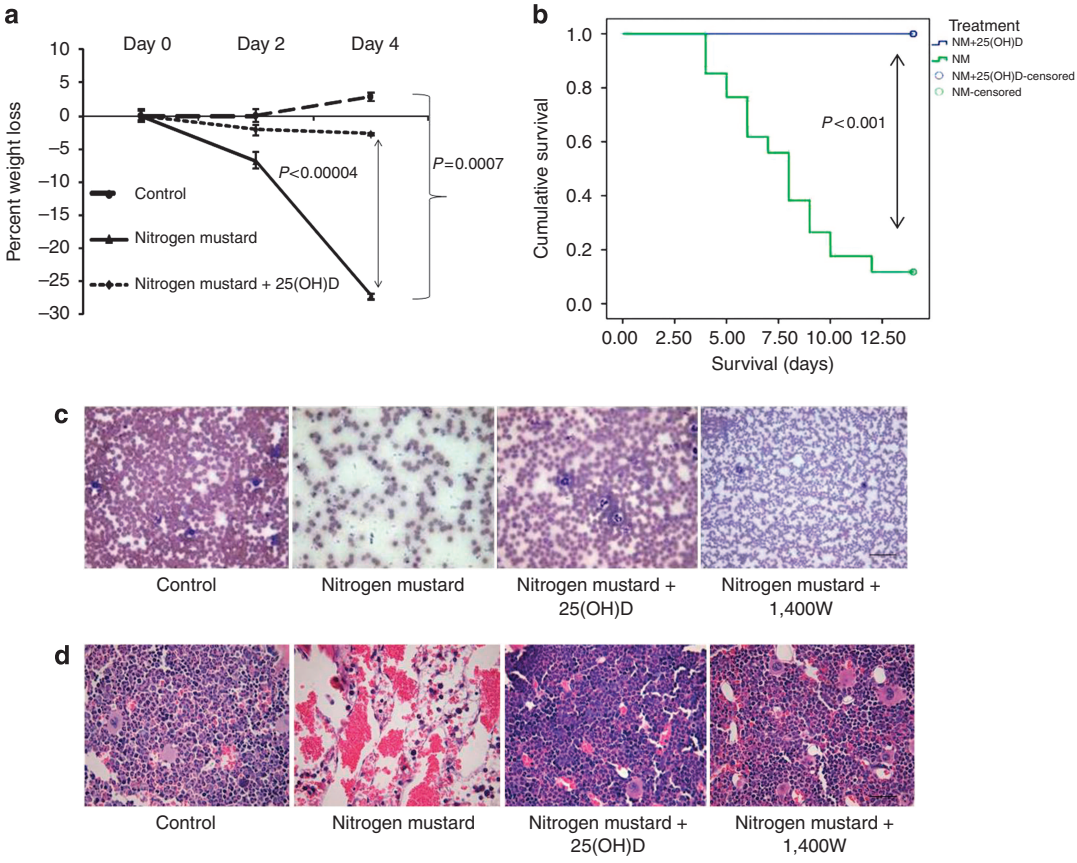

Figure 2. 25(OH)D prevents systemic toxicity and mortality in C57BL/6 mice subsequent to topical application of NM. C57BL/6 mice were subjected to wound formation by cutaneous exposure to NM followed by a systemic dose of 25(OH)D. (**a**) Mice were weighed to record percentage loss in body weight up to day 4 ($n = 6$, $P < 0.0007$) (**b**) Kaplan–Meier survival curve was plotted up to day 13. Censored refers to animals that were alive at the end of the study. *P*-values are determined by log-rank test ($n = 34$ for NM, $n = 22$ (NM+25OHD), $P < 0.001$). Five days following NM exposure mice were killed and sternum and blood collected for analyses of (**c**) Peripheral blood smears, (**d**) H&E sections of sternums in presence and absence of 25(OH)D. All data presented as means ± SEM. Scale Bar = 100 μm.

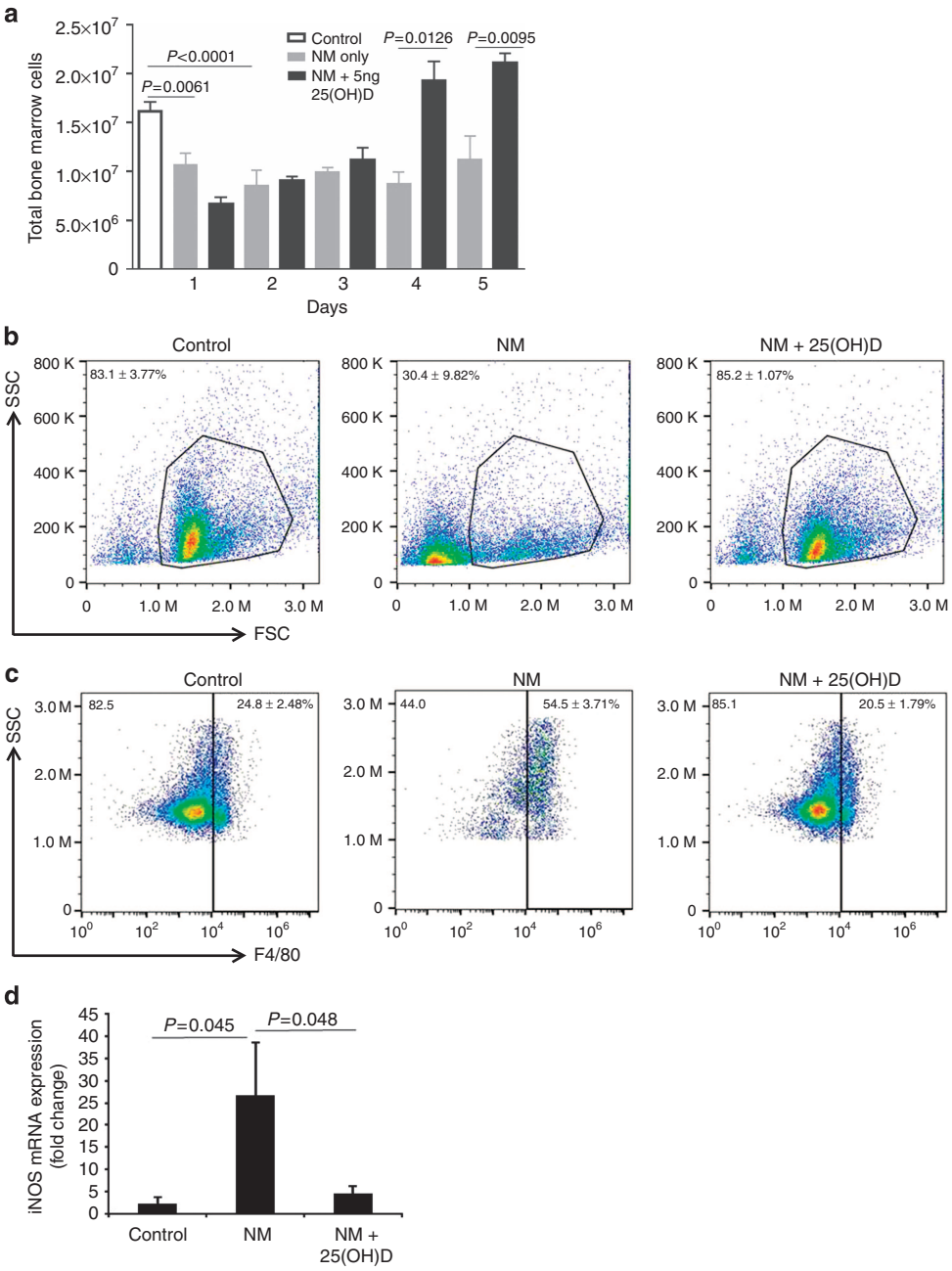

Figure 3. 25(OH)D facilitates recovery of BM cellularity of NM exposed mice with decrease of iNOS expression. (**a**) Total BM cell counts were recorded daily for 5 days following NM exposure in presence and absence of 25(OH)D. Bone marrow cells were isolated on day 5 for characterization (**b**) Representative FSC-SSC flow cytometric scatter plots of viable nucleated BM cells ($n=3$, $P=0.007$ control vs. NM, $P=0.005$ NM vs. NM+25(OH)D), (**c**) Percentage of F4/80$^+$ macrophages in control, NM and NM+25(OH)D-treated mice ($n=6$, $P<0.002$ control vs. NM, $P<0.0004$ for NM vs. NM+25(OH)D). (**d**) BM-derived iNOS mRNA levels were evaluated ($n=8$; $P<0.05$). All data presented as means ± SEM.

baseline levels (Figure 3c), with increased absolute numbers indicating an overall recovery of cells in the marrow (Supplementary Figure S3 online). On the basis of the observation that skin inflammation and necrosis were exacerbated with elevated iNOS from F4/80+ macrophages we next examined whether NM-induced disruption of BM was similarly associated with increased iNOS. A robust 26-fold increase in iNOS mRNA expression in NM-exposed mice was observed that was significantly suppressed with 25(OH)D intervention (Figure 3d).

Inflammatory macrophages from skin promote BM disruption

Given that iNOS expression is inextricably linked to macrophages, we tested the hypothesis that skin macrophages may be tracking to the BM to contribute to high expression of iNOS. Liposome-encapsulated dialkylcarbocyanine dye (DiI)

was injected subcutaneously at the wound site to allow for its phagocytosis by skin macrophages thus enabling localization. Five days post NM exposure, sternum sections were examined for iNOS producing dermal activated macrophages. Using confocal microscopy, we triple co-localized a small population of F4/80+DiI+iNOS+ macrophages in the sternum (Figure 4a). Treatment with 25(OH)D strongly reduced iNOS expression and detected a large population of F4/80+ DiI− iNOS− macrophages, consistent with the BM cellular recovery process from 25(OH)D intervention. Flow cytometric analysis confirmed the increased percentage of F4/80+DiI+ BM macrophages compared with that found in NM+25(OH)D-mice (8.31 ± 1.74% vs. 1.42 ± 0.23%; Figure 4b). Quantification of absolute cell numbers in NM mice injected with DiI show increased F4/80+DiI+ macrophages with a modest increase in F4/80+/DiI− cells (Figure 4c and d). In contrast, mice treated with 25(OH)D demonstrate no significant increase in F4/80+DiI+ macrophages with a concurrent significant increase in F4/80+/DiI− macrophages (Figure 4c and d). We next used complimentary imaging techniques to confirm the presence of skin macrophages in the BM. Mice were injected subcutaneously with a pH-dependent fluorescent dye conjugated with bacteria (pHrodo) at the NM wound area to allow for phagocytosis by infiltrating macrophages (Aziz *et al.*, 2013; Miksa *et al.*, 2009). Following phagocytosis, pHrodo is activated by the acidic pH within phagolysosomes of macrophages resulting in emission of a wavelength that can be visualized by Maestro imaging of whole organs. Consistent with the DiI labeling studies, 5 days following NM skin exposure, the sternum of mice demonstrated marked increase in fluorescence of pHrodo compared with controls and mice treated with 25(OH)D (Figure 4e). Cumulatively these data confirm that the increase of activated iNOS-expressing macrophages localized in the marrow of NM mice originate partly from inflamed injured skin. This increase in F4/80+/DiI+ macrophages in BM on day 5 is unique to NM exposure and cannot be solely attributed to passive transfer of labeling agents from increased vascular permeability, as compared with other models of inflamed skin using UVR, mechanical tape-stripping, or chemical injury with depilating agents (Supplementary Figure S4 online).

Dermally activated macrophages contribute to NM-mediated pathology in the BM

To confirm that dermally derived macrophages contribute to exacerbated pathology observed in the marrow, liposome-encapsulated clodronate was injected at the site of the skin wound. Compared with NM mice injected with control PBS liposome, depletion of skin macrophages with clodronate liposome resulted in decreased percentage of F4/80+ macrophages in BM (Figure 5a) with a corresponding reduction in iNOS expression. (Figure 5b). In addition, liposomal clodronate-treated animals demonstrated rapid cellular recovery, maintenance of body weight (Figure 5c), restoration of CBC values comparable to healthy controls by day 5 (Table 2) correlating with histological images of the sternum presenting recovery of the BM (Figure 5d).

To exclude that appearance of dermal DiI labeled macrophages in the BM as a result of cellular leakage from inflamed capillaries in NM mice, the BM was examined at earlier time points. Day 2 post NM exposure shows non-significant changes in F4/80+DiI+ macrophages in the marrow across all conditions (Figure 5e) with significance observed only on day 5 (Figure 5e and f). We further performed co-injection experiments with liposomal DiI and liposomal clodronate at the NM wound site to deplete local skin macrophages and further exclude the possibility of systemic distribution of DiI. Sternum sections on days 2 and 5 post exposure reveal significantly diminished F4/80+DiI+ cells in liposomal clodronate-treated animals, consistent with our previous observation of cellular recovery of the marrow in the absence of activated pathogenic dermal macrophages (Figure 5e and f). Taken together, these experiments suggest that the appearance of DiI labeled cells on day 5 is not due to increased cellular leakage but marks a specific homing of macrophages back to the marrow.

DISCUSSION

NM is a chemical agent that has recently come under the purview of intense investigation mostly due to its DNA alkylating property in the treatment of multiple diseases including childhood and adult cancers (Shepherd and Harrap, 1982; Sharma *et al.*, 2010a). Treatment of skin diseases such as mycosis fungoides with topical NM has been in practice for over five decades (Haserick, 1983) with response rates reported to be 83% of patients with early stage disease (Chung *et al.*, 2003). The amount of NM that patients are exposed to varies according to frequency of application, amount of body surface area treated, and differing formulations of topical preparations with only recent FDA approval of a 0.02% gel formula (Talpur *et al.*, 2014). Nonetheless, adverse skin reactions in 30–80% cases are the most common side effects, with intolerance requiring cessation of therapy in some patients (de Quatrebarbes *et al.*, 2005). Clinically, treatment of leukemia and refractory lymphoma with NM derivatives such as nitrosourea or bendamustine is limited by dose-dependent toxicity where patients exhibit signs of myelosuppression characterized by anemia and neutropenia early in treatment followed by thrombocytopenia at later time points (Bertoncello *et al.*, 1988; (Heimfeld *et al.*, 1991; Zaja *et al.*, 2013). Whereas studies have demonstrated that cutaneous exposure to NM causes acute skin injury leading to vesication, little has been studied on the mechanism of systemic toxicity following breach of the skin epithelial barrier. Consistent with previous reports our study demonstrates that pharmacologic inhibition of iNOS using compound 1400W conferred protection to mice from NM-induced tissue injury and attenuated local and systemic tissue destruction (O'Neill *et al.*, 2011; Sunil *et al.*, 2012). Furthermore, our study demonstrates that vitamin D, a safe and well tolerated drug, accelerates wound healing and promotes recovery from NM-induced disruption of hematopoiesis potentially by augmenting host immune responses. These findings have translational potential in

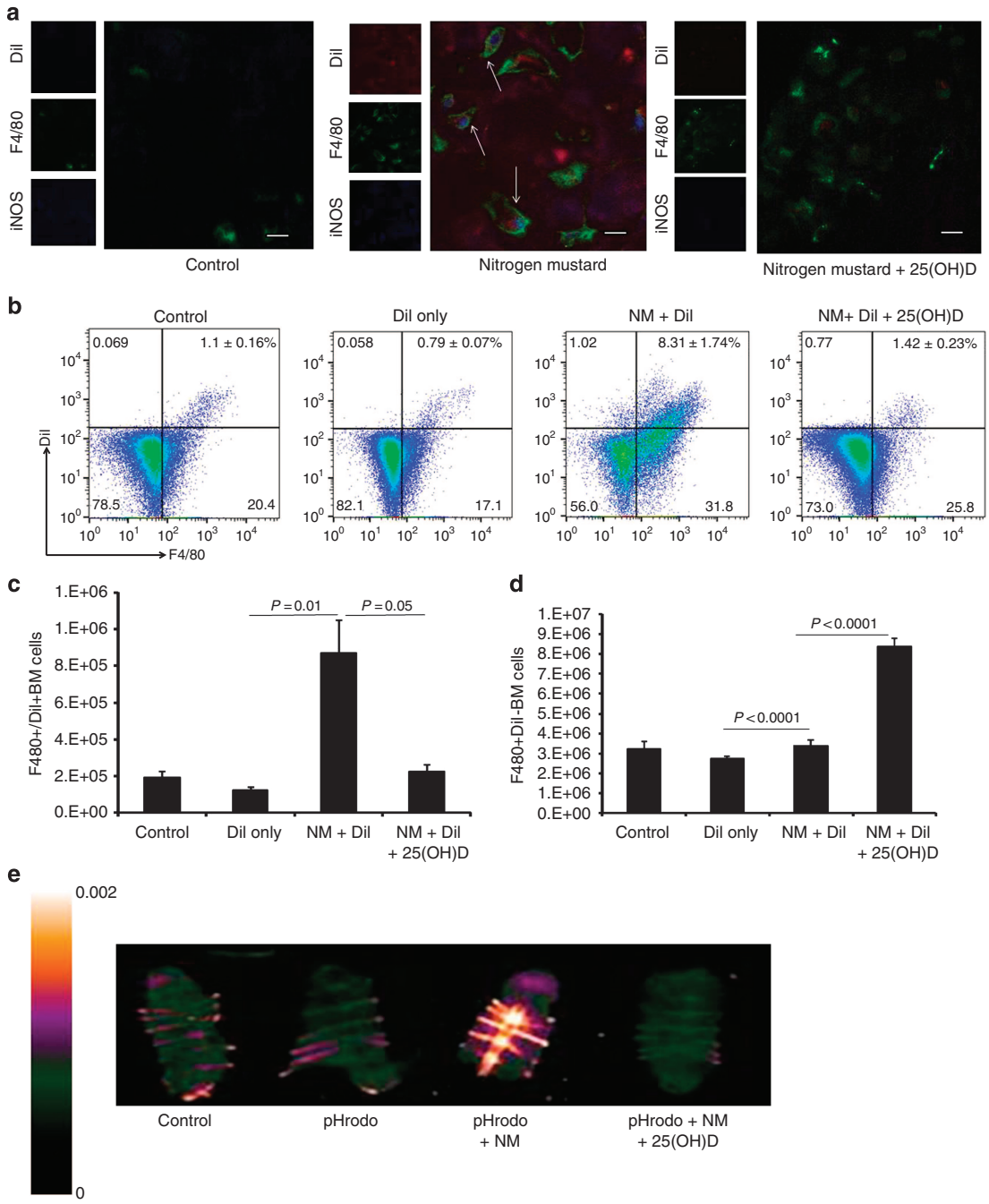

Figure 4. Appearance of dermal hyperactivated macrophages in the BM after topical NM exposure. NM-exposed mice were injected intradermally with DiI post NM exposure with and without 25(OH)D. (**a**) Sternums were sectioned for co-localization of DiI (red), iNOS (blue) and F4/80$^+$ (green) macrophages in the marrow (arrows) by confocal microscopy. Bone marrow cells were subjected to flow cytometric analysis (**b**) to detect F4/80+DiI+ and F480+DiI− macrophages, and for quantitative analysis of absolute cell numbers of (**c**) F4/80+ DiI+ cells ($n = 4$; $P = 0.01$, $P = 0.05$) and (**d**) F4/80+DiI− cells ($P < 0.0001$). pHrodo dye conjugated with bacteria was injected subcutaneously at the wound site 1 hour following NM exposure to detect (**e**) pHrodo-derived fluorescence in the sternum of NM-exposed mice 5 days after injection as visualized by Maestro imaging. Scale Bar = 100 μm.

ameliorating the unwanted adverse effects for cancer patients undergoing treatment with NM and NM derivatives.

The observation that calcitriol inhibits NFκB, a critical transcription factor for TNFα and iNOS expression, prompted treatment with 25(OH)D as a countermeasure for macrophage activation following vesicant-induced skin injury (Mahon *et al.*, 2003; Di Rosa *et al.*, 2012). The deleterious effect of dysregulated macrophages is not restricted to skin injury but has also played a critical role in other organ injuries, including the lungs and liver. In this study we focus on skin

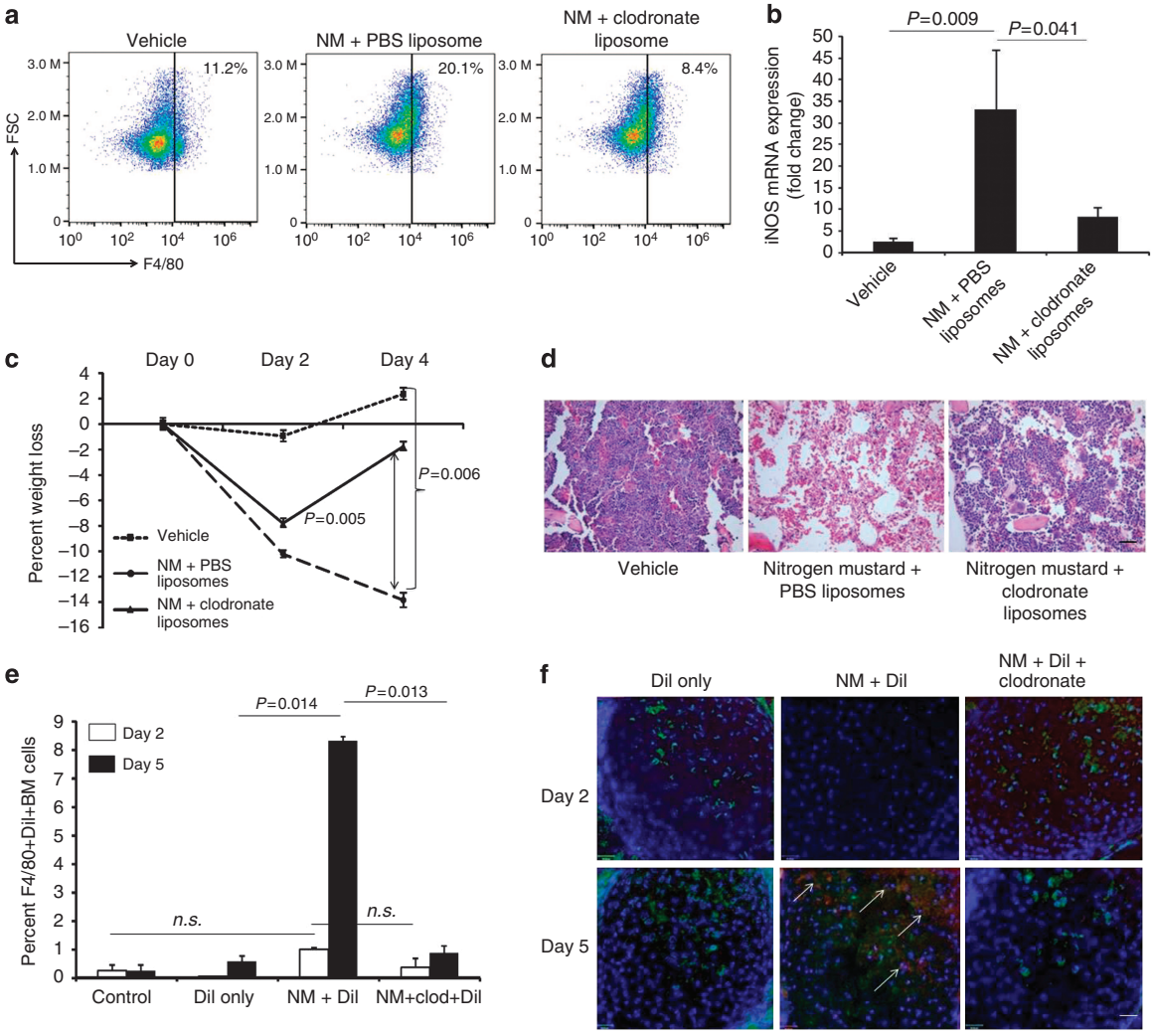

Figure 5. Dermally activated macrophages contribute to NM-mediated pathology in the bone marrow. Dermal macrophages were depleted by clodronate injection 1 hour following topical application of NM. Five days post exposure bone marrow cells were isolated from mice injected with PBS-liposome (vehicle), NM+PBS-liposome and NM+Clodronate liposome for (**a**) detection of F4/80+ macrophages by flow cytometry, and (**b**) iNOS mRNA expression by qPCR ($n=5$, $P=0.009$, $P=0.041$). (**c**) Percentage body weight loss recorded ($n=6$; $P<0.006$), (**d**) H&E staining of sternum 5 days post exposure. DiI+clodronate co-injection experiments were conducted on NM-exposed mice. (**e**) Percent F4/80+DiI+ BM cells quantified by flow cytometry at days 2 and 5 post exposure to mustard. (**f**) Detection of F480+DiI+ macrophages by confocal microscopy. All data presented as means ± SEM. Scale Bar = 100 μm.

Table 2. CBC analyses of clodronate treated mice on day 5 post NM exposure ($n=8$)

	Vehicle	NM+PBS Liposomes	NM+Clodronate Liposomes
WBC ($\times 10^3\ \mu l^{-1}$)	7.77 ± 0.83	3.88 ± 0.76*	6.57 ± 0.41#
LYM ($\times 10^3\ \mu l^{-1}$)	5.93 ± 0.61	2.82 ± 0.53*	4.64 ± 0.30#
MONO ($\times 10^3\ \mu l^{-1}$)	0.46 ± 0.06	0.28 ± 0.54*	0.48 ± 0.05
GRAN ($\times 10^3\ \mu l^{-1}$)	1.39 ± 0.22	0.78. ± 0.19*	1.46 ± 0.12#
HCT (%)	38.5 ± 3.53	23.6 ± 2.74*	30.49 ± 2.15
HGB ($g\ dl^{-1}$)	13.7 ± 1.08	8.52 ± 0.93*	11.06 ± 0.63#

Abbreviations: CBC, complete blood count; GRAN, granulocytes; HCT, hematocrit; HGB, hemoglobin; LYM, lymphocytes; MONO, monocytes; NM, nitrogen mustard; PBS, phosphate-buffered saline; WBC, white blood cell.
*$P<0.01$, #$P<0.04$.

injury and demonstrate that hyper-activated macrophages from skin contribute to disruption of hematopoiesis in the BM. Our results demonstrate that a single dose of systemically administered 25(OH)D is sufficient to reduce skin inflammation and necrosis and accelerate wound healing subsequent to topical application of NM. Repeated dosing of vitamin D may improve outcome of other epithelial surfaces or vital organs that are vulnerable to NM exposure. In our experimental model, the contribution of other innate immune cells such as neutrophils acting at earlier time points cannot be eliminated as neutrophils are rapid responders in skin injury and may have a role in amplifying macrophage accumulation in the skin (Wilgus *et al.*, 2013).

Intervention with 25(OH)D rescued mice from local and systemic pathology by mitigating the activation of the host immune system characterized by elevation of dysregulated expression of reactive species mostly in macrophages (Laskin and Laskin, 1996; Korkmaz *et al.*, 2006). Work by Correa–Costa is consistent with our findings that macrophage depletion using clodronate ensures substantial protection from organ damage in a tubulo-interstitial nephritis model (Correa-Costa *et al.*, 2014). Thus in addition to direct toxicity of NM, our study demonstrates that local NM exposure provokes an immune reactive response that delays local healing and exacerbates systemic pathology. The appearance of skin-labeled macrophages in the marrow at later time points cannot be explained solely by passive migration of macrophages due to increased skin permeability. Compared with other models of skin injury, only NM exposure induces translocation of skin labeled macrophages in the marrow. Our studies show that the damage in BM is rapid, presumably via direct toxic effects of NM, resulting in decreased cell counts as early as 24 hours. This initial damage to the marrow may provide a chemotactic signal for inflammatory tissue macrophages to infiltrate the BM where they further promote tissue destruction or suppress recovery. Using 25(OH)D or liposomal clodronate intervention in the BM recovery process, we delineate the small subset of inflammatory tissue macrophages to be distinct from macrophages and monocytes within the BM and future studies will focus on further phenotyping this cell population.

In summary, these data reveal a critical role for cutaneous activated macrophages in tissue destruction and immune activation and as a link between local and systemic pathogenic responses following NM exposure. Vitamin D-related compounds have the potential to be developed as a therapy for mitigating the unwanted toxic effects of mustard agents.

MATERIALS AND METHODS

Mice

Six to eight-week-old pathogen-free female C57BL/6J mice and *nos*2 knockout mice were obtained from Jackson Laboratories (Bar Harbor, ME). All animals received standard laboratory diet. All animal studies have been approved by Case Western Reserve Institutional Animal Care and Committee. Under BSL2 guidelines, all mice were caged individually for experiments in one-time use disposable polystyrene cages.

NM application

NM $(ClCH_2CH_2)2NCH_3 \times HCl$ was obtained from Sigma-Aldrich Chemical Company (St Louis, MO). For generating skin wounds, mice were anesthetized by intraperitoneal injection of avertin, the dorsal fur removed with clippers and depilating cream and 48 hours later NM (20 ul of a 2.0% solution in 1X PBS) was applied over a circular template of 8 mm diameter measuring about 50 mm^2 area on the dorsal surface of each mouse. Following recovery from anesthesia during which time the applied NM is completely absorbed into the skin.

Local inflammation on skin

Local inflammation including erythema of skin was induced by three methods–tape stripping, UVR and chemical injury using depilating agent. Following hair depilation as described before, mice were anesthetized and tape stripping was performed by using 10 strokes of duct tape as described (Guiducci *et al.*, 2010), or exposed to a submaximal dose of 100 mJ of UV (Toichi *et al.*, 2008), (Metz *et al.*, 2006), or subject to a hair depilating agent smeared on their shaved backs for 24 minutes to induce inflammation from chemical injury (Angel *et al.*, 1992), (Karegoudar *et al.*, 2012).

Vitamin D

25(OH)D (Sigma-Aldrich) was reconstituted in ethanol and diluted in mineral oil for intraperitoneal injections at 5 ng of 25(OH)D, 1 hour following NM exposure.

1400W

1400W (hydrochloride) (Sigma-Aldrich) was reconstituted in ethanol and diluted in 1X PBS. 10 mg kg^{-1} of 1400W were injected intraperitoneally 1 hour following NM exposure.

Wound and weight measurements

Wounds were measured with a digital caliper every other day by length and width inside the 50 mm^2 circular template. Weights were recorded every other day using a Model CS 200 scale (Ohaus Corporation, Parsipanny, NJ).

Realtime PCR

RNA was isolated using Trizol (Invitrogen, Carlsbad, CA) following manufacturer's instructions. RNA (100 ng) was used for quantification of TNF-α, iNOS mRNA expression using TaqMan Gene Expression Assays and the Taqman RNA-to-C_T 1-Step (Life Technologies, Grand Island, NY). Samples were analyzed using a Step-One System (Applied Biosystems, Grand Island, NY) based on manufacturer's recommendations. Gene expression was expressed as fold changes normalized to the 18S RNA housekeeping gene.

Blood smear

A drop of blood was collected on a glass slide following tail snip, smeared using a microscope slide, fixed in 100% methanol, and stained with Wright–Giemsa to observe cell types.

H&E staining of bone marrow

Sternums were removed and fixed overnight in 10% formalin diluted in PBS. Samples were embedded in paraffin, sectioned, and stained with hematoxylin and eosin.

Complete blood count

Blood (20 ul) was obtained in an EDTA coated capillary tube following tail snip. CBC were determined using a HemaTrue Hematology Analyzer (Heska Corporation, Loveland, CO) at the Mouse Physiology Phenotyping Center at Case Western Reserve University.

Immunofluorescence staining

For immunofluorescence staining of skin and sternum OCT-embedded sections were sectioned 8 μm thick and subjected to staining as described before (Das *et al.*, 2014). Primary antibodies used in 10% goat serum are the following: anti-mouse F4/80 antigen Alexa-488; rat IgG2a isotype—Alexa 488 (eBioscience, SanDiego, CA, 1:100); rabbit-anti-mouse iNOS (Upstate Temecula, CA); isotype rabbit IgG (R&D Systems, Minneapolis, MN). Secondary antibodies: goat anti-rabbit Alexa Fluor 647 conjugated (1:2,000 in 1X PBS) (Life Technologies). Labeled sections were imaged using a UltraVIEW VoX spinning disk confocal microscope (Leica DMI6000B).

Flow cytometry

Tibiae and femurs of mice were isolated by removing skin and soft tissue. BM cells were isolated as described before (Horak *et al.*, 1983), stained with rat anti-mouse F4/80 Ab or rat IgG2a isotype (Alexa Fluor488) and analyzed by Accuri C6 flow cytometer with fluorescence detected on the FL1 channel.

Liposomes

Liposomes (obtained through www.clodronateliposomes.org, Amsterdam, Netherlands) suspended in 1X PBS (pH 7.4) were loaded with either PBS, clodronate or the DiI dye. Mice received subcutaneous injections of PBS-liposomes for control, clodronate-liposomes or DiI-liposomes 1 hour after NM application on the 50 mm^2 dorsal region onto which NM was applied.

Co-injection studies

NM mice were subjected to 200 ul intradermal injection of a 1:1 mixture of liposomal clodronate and liposomal DiI at the doses indicated above, 1 hour following NM exposure. Two and five days post exposure mice were killed for detection of F4/80+DiI+ macrophages in the BM. and sternums sectioned for colocalization of DiI (red) and F4/80 (green) macrophages. DAPI (blue) stained for cellular nuclei.

Maestro imaging

The *Escherichia coli*-conjugated pHrodo dye (Life Technologies) was injected subcutaneously at the wound site 1 hour post NM. Five days later, the biodistribution of pHrodo in the sternums of mice was analyzed using Maestro fluorescence imaging with green excitation (503–548 nm) and emission (560 nm longpass) filters and a 5,000 ms exposure time.

Statistical analysis

A two-sided unpaired Student's *t*-test was used to determine statistical significance. Data are shown as mean ± SEM, and *P*-values ≤ 0.05 were considered statistically significant. The Kaplan–Meier method was used to plot the survival distributions of the two groups (NM and NM+25(OH)D), which were then compared using the log-rank test.

CONFLICT OF INTEREST

The authors state no conflict of interest.

ACKNOWLEDGMENTS

We thank KD Cooper and TS McCormick for critical discussions and reading of the manuscript; K Honda, G Jacobs, L Sandhaus, M Cohens, and T Bonfield for H&E tissue slide analysis; Skin Disease Research Center at Case Western Reserve University; Sara Debanne for assistance with statistical analysis with survival data. This work was funded by the National Institute of Arthritis Musculoskeletal and Skin Diseases (P30-AR039750); National Institute of Health (U01-AR064144).

Author contributions

LA and JPM, conducted most experiments constituting the manuscript. AMB and AMW conducted key experimental assays including the fluorescent imaging and replicates of survival studies. RSB contributed to 25(OH)D dose determination and administration. NFS contributed her expertise in designing the whole organ imaging studies involving DiI and pHrodo. LMD prepared and wrote the manuscript. KQL was responsible for conceiving the study and designing the experiments.

SUPPLEMENTARY MATERIAL

Supplementary material is linked to the online version of the paper at http://www.nature.com/jid

REFERENCES

Bertoncello I, Hodgson GS, Bradley TR (1988) Multiparameter analysis of transplantable hemopoietic stem cells. II. Stem cells of long-term bone marrow-reconstituted recipients. *Exp Hematol* 16:245–9

Bogdan C (2001) Nitric oxide and the immune response. *Nat Immunol* 2: 907–16

Chen Y, Kong J, Sun T *et al.* (2011) 1,25-Dihydroxyvitamin D(3) suppresses inflammation-induced expression of plasminogen activator inhibitor-1 by blocking nuclear factor-kappaB activation. *Arch Biochem Biophys* 507: 241–7

Correa-Costa M, Braga TT, Felizardo RJ *et al.* (2014) Macrophage trafficking as key mediator of adenine-induced kidney injury. *Mediators Inflamm* 2014: 291024

Das LM, Rosenjack J, Au L *et al.* (2014) Hyper-inflammation and skin destruction mediated by rosiglitazone activation of macrophages in IL-6 deficiency. *J Invest Dermatol* 135:389–99

DeVita VT Jr, Chu E (2008) A history of cancer chemotherapy. *Cancer Res* 68: 8643–53

Di Rosa M, Malaguarnera G, De Gregorio C *et al.* (2012) Immuno-modulatory effects of vitamin D3 in human monocyte and macrophages. *Cell Immunol* 280:36–43

Gunnarsson PO, Andersson SB, Sandberg AA *et al.* (1991) Accumulation of estramustine and estromustine in adipose tissue of rats and humans. *Cancer Chemother Pharmacol* 28:361–4

Heimfeld S, Hudak S, Weissman I *et al.* (1991) The in vitro response of phenotypically defined mouse stem cells and myeloerythroid progenitors to single or multiple growth factors. *Proc Natl Acad Sci USA* 88:9902–6

Holick MF (1993) Active vitamin D compounds and analogues: a new therapeutic era for dermatology in the 21st century. *Mayo Clin Proc* 68: 925–7

Holick MF (2003) Vitamin D: a millenium perspective. *J Cell Biochem* 88: 296–307

Jain AK, Tewari-Singh N, Inturi S *et al.* (2014) Myeloperoxidase deficiency attenuates nitrogen mustard-induced skin injuries. *Toxicology* 320:25–33

Keramati MR, Balali-Mood M, Mousavi SR *et al.* (2013) Biochemical and hematological findings of Khorasan veterans 23 years after sulfur mustard exposure. *J Res Med Sci* 18:855–9

Kondo T, Ishida Y (2010) Molecular pathology of wound healing. *Forensic Sci Int* 203:93–8

Korkmaz A, Yaren H, Topal T *et al.* (2006) Molecular targets against mustard toxicity: implication of cell surface receptors, peroxynitrite production, and PARP activation. *Arch Toxicol* 80:662–70

Lagishetty V, Liu NQ, Hewison M (2011) Vitamin D metabolism and innate immunity. *Mol Cell Endocrinol* 347:97–105

Laskin DL, Heck DE, Punjabi CJ *et al.* (1996a) Role of nitric oxide in hematosuppression and benzene-induced toxicity. *Environ Health Perspect* 104(Suppl 6):1283–7

Laskin DL, Laskin JD (1996) Macrophages, inflammatory mediators, and lung injury. *Methods* 10:61–70

Laskin JD, Heck DE, Laskin DL (1996b) Nitric oxide production in the lung and liver following inhalation of the pulmonary irritant ozone. *Adv Exp Med Biol* 387:141–6

Mahon BD, Wittke A, Weaver V *et al.* (2003) The targets of vitamin D depend on the differentiation and activation status of CD4 positive T cells. *J Cell Biochem* 89:922–32

Malaviya R, Venosa A, Hall L *et al.* (2012) Attenuation of acute nitrogen mustard-induced lung injury, inflammation and fibrogenesis by a nitric oxide synthase inhibitor. *Toxicol Appl Pharmacol* 265:279–91

Miksa M, Komura H, Wu R *et al.* (2009) A novel method to determine the engulfment of apoptotic cells by macrophages using pHrodo succinimidyl ester. *J Immunol Methods* 342:71–7

Mora JR, Iwata M, von Andrian UH (2008) Vitamin effects on the immune system: vitamins A and D take centre stage. *Nat Rev Immunol* 8: 685–98

O'Neill HC, Orlicky DJ, Hendry-Hofer TB *et al.* (2011) Role of reactive oxygen and nitrogen species in olfactory epithelial injury by the sulfur mustard analogue 2-chloroethyl ethyl sulfide. *Am J Respir Cell Mol Biol* 45: 323–31

Pearson C (2006) The Role of Chemistry in History. http://itech.dickinson.edu/chemistry/?p=408

Requena L, Requena C, Sanchez M *et al.* (1988) Chemical warfare. Cutaneous lesions from mustard gas. *J Am Acad Dermatol* 19:529–36

Schein PS, Green D, Dean SW *et al.* (1987) 6-[Bis(2-chloroethyl)amino]-6-deoxygalactopyranose hydrochloride (C6-galactose mustard), a new alkylating agent with reduced bone marrow toxicity. *Cancer Res* 47: 696–9

Sharma M, Pant SC, Pant JC *et al.* (2010a) Nitrogen and sulphur mustard induced histopathological observations in mouse visceral organs. *J Environ Biol* 31:891–905

Sharma M, Vijayaraghavan R, Agrawal OP (2010b) Comparative toxic effect of nitrogen mustards (HN-1, HN-2, and HN-3) and sulfur mustard on hematological and biochemical variables and their protection by DRDE-07 and its analogues. *Int J Toxicol* 29:391–401

Shepherd R, Harrap KR (1982) Modulation of the toxicity and antitumour activity of alkylating drugs by steroids. *Br J Cancer* 45:413–20

Sunil VR, Shen J, Patel-Vayas K *et al.* (2012) Role of reactive nitrogen species generated via inducible nitric oxide synthase in vesicant-induced lung injury, inflammation and altered lung functioning. *Toxicol Appl Pharmacol* 261:22–30

Ward NL, Loyd CM, Wolfram JA *et al.* (2011) Depletion of antigen-presenting cells by clodronate liposomes reverses the psoriatic skin phenotype in KC-Tie2 mice. *Br J Dermatol* 164:750–8

Yaren H, Mollaoglu H, Kurt B *et al.* (2007) Lung toxicity of nitrogen mustard may be mediated by nitric oxide and peroxynitrite in rats. *Res Vet Sci* 83:116–22

Zheng R, Po I, Mishin V *et al.* (2013) The generation of 4-hydroxynonenal, an electrophilic lipid peroxidation end product, in rabbit cornea organ cultures treated with UVB light and nitrogen mustard. *Toxicol Appl Pharmacol* 272:345–55